Vol.5 No.1 Jan. 2024
Multimedia Research (MR)
Received 3 September, Revised 11 November, Accepted 31 December

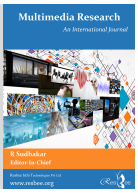

Hybrid Particle Swarm Optimization and Jaya Optimization Algorithm based CNN for HEp-2 Cell Classification

Srinivas Kongara
Associate Manager LKM , Accenture (India).

Abstract: In human serum, Anti Nuclear Antibodies (ANA) are present which have a connection with several autoimmune diseases. In order to diagnose these autoimmune diseases, the HEp-2 cells perform as a substance in the IIF test. Recently, using the HEp-2 cell classification, the computer-aided diagnosis of autoimmune diseases received huge attention. Though, they frequently pretense restrictions such as small inter-class as well as large intra-class deviations. Therefore, several attempts are carried out to computerize the process of HEp-2 cell classification. To surmount the aforesaid issues, this paper proposes a novel HEp-2 classification procedure. Here, it is worked by means of integration of two procedures such as classification and segmentation. At first, HEp-2 cells segmentation is performed using morphological operations. In this work, this is regulated using two morphological operations such as opening well as closing. Furthermore, the Convolutional Neural Network (CNN) is used for the classification process. Here, the most important contribution is the classification of HEp-2 cells effectively (Golgi, Centromere, Nucleolar, NuMem, Homogeneous, as well as Speckled) it is performed using the optimization model. Here, a novel optimization approach is named Hybrid Particle Swarm Optimization and Jaya Optimization Algorithm (Hybrid PSO-JA) that chooses the optimal convolutional layer in CNN. At last, the performance evaluation is performed by evaluating the proposed model with the other existing approaches regarding the positive as well as negative measures.

Keywords: Classifications, Human Epithelial Type-2 Indirect Immuno Fluorescence, Morphological Operations, Optimization Algorithm

Nomenclature

Abbreviations	Descriptions
IIF	Immunofluorescence Image Analysis Systems
IR	Ionizing Radiation
CNN's	Convolutional Neural Networks
CXCL10	CXC chemokine ligand 10
C. Albicans	Candida albicans
VHAR	Vector of Hierarchically Aggregated Residuals
IIF	Immunofluorescence Image Analysis Systems
IR	Ionizing Radiation
CNN's	Convolutional Neural Networks

1. Introduction

In Indirect IIF, the cell images of HEp-2 patterns evaluation is considered a noteworthy task in detecting autoimmune diseases of humans. Here, the specimen cells of HEp-2 are categorized into seven classifications such as nuclear membrane, centromere, nucleolar, Speckled, Golgi, homogeneous, as well as the mitotic spindle. Different staining patterns can be produced by the HEp-2 test due to the diverse cell domains or regions that are stained. The cell structure comprises chromosomes, nucleoli, nucleus, and cytoplasm that may vary in number, shape, position, and size within the cell. This aids researchers to distinguish the characteristic of staining patterns for diverse autoimmune diseases. Nevertheless, manual recognition of Hep-2 cell images multiple cells in a laboratory is a complicated procedure due it is time utilization as well as needs enormous efforts from professionals. Moreover, more than two experts would be needed for each sample inspection because of inter-observer variability.

Over the decades, by IIF, HEp-2 cells analysis has been performed both automatically as well as manually however these processes are prejudiced as well as time utilizing. To handle raising cell data

volumes, Hand-engineered technologies are unable which is produced them on the basis of everyday life, producing them more and more high-priced. Likely to be a very good technique to satisfy this requirement for both the scalable as well as automated techniques is an advancement of computer-aided diagnosis systems on the basis of the machine learning and image processing approaches.

Machine learning, as well as Digital Image processing, is important for a huge amount of computer assistive diagnosis applications. Each day, novel HEp-two cells IIF images are formed universally, producing huge datasets. Generally, solutions on the basis of the analysis of computerized images possess a minimum cost as well as highly autonomous, as data and outcomes of analysis might be shared as well as reprocessed over the globe. This feature makes such models financially eye-catching, particularly for rising nations. The gathering of enormous numbers of data, as well as particularly in images form, has permitted deep learning models to turn out to be successful. Especially, CNNs have shown effectual outcomes in broad visual recognition tasks, inspiring their extensive application in numerous research areas.

In numerous studies, Machine Learning models were presented to mechanize the process of HEp-2 cell classification as well as generate more objective characterizations. From IIF images these techniques, use visual features extracted that are exploited to train a classification method to differentiate amid numerous classes on the basis of example images.

The main aim of this research is to develop a novel HEp-2 classification using two procedures named classification well as segmentation. Initially, by exploiting two morphological operators such as opening and closing, the segmentation is carried out. Subsequently, using the enhanced CNN, the HEp-2 cell classification is performed. The most important contribution is regarding the classification rate, and it is achieved by using a novel enhanced approach, called Hybrid PSO-JA. The approach chooses the optimal convolutional layer in CNN which shows the method for effectual and accurate classification outcome. Finally, the proposed model performance is evaluated with the existing approaches regarding various metrics.

2. Literature Review

In 2021, Yunting Lin et al [1], worked on the sensitivities of diverse tumor cells to radiation as well as ascertained HEp-2 cells as radio-resistant tumor cells for additional examination. The most important host immune response regulator was IFN gamma exhibited the possibility to sensitize tumors to IR. Moreover, it was necessary for the effectual IR-induced killing of cultured HEP-2 cells; IFNgamma-induced CXCL10 was established. In CXCL10-KO cells as well as CXCL10-depleted HEp-2 cells, the maximized clonogenic survival was seen. In addition, in HEp-2 cells, the CXCL10 loss exhibited less progression of the G0/G1 stage to G2/M while showing to IR (8 Gy).

In 2019, Zohreh Khodaii et al [2], worked on the examination of the aqueous extracts of Punica granatum, Eugenia caryophyllata, Rhus coriaria, and Cichorium intybus, as anti-adhesion agents of C. Albicans to HEp-2 cells. By exploiting two techniques such as a standard agar well diffusion assay and observing C. Albicans growth, anti- C. Albicans activity of extracts was estimated in attendance of extracts through optical density. By exploiting MTT assay the cytotoxic concentrations of the attained aqueous extracts over HEp-2 cells were evaluated.

In 2019, Khamael Al-Dulaimi et al [3], focused on the HEp-2 specimen cell classification task regarding the features selection, feature extraction indications, and classifier model. A linear discriminant analysis technique was modeled from a segmented HEp-2 specimen cell, a shape that relies on bispectral invariant features which permit simplifying features to being deviations in rotation, shape, scaling as well as shifting. In geometric active contours and normal direction, the HEp-2 specimen cell was ascertained by exploiting the level set-based forces.

In 2019, Larissa Ferreira Rodrigues et al [4] studied the six preprocessing schemes performance and five conventional CNN models for the classification of the HEp-2 cell. Here, the improvement techniques were evaluated namely, data augmentation, hyper-parameter optimization as well fine-tuning schemes. By exploiting fivefold cross-validation processes, every experiment was examined against the test as well as training sets. Regarding the accuracy, the optimal outcomes were attained by training the examination V3 technique from the scratch.

In 2017, Dimitris Kastaniotis et al [5], focused on the HEp-2 cell classification so a new model was adopted for local features that encode and permit simplifying the remaining idea in the encoding of sparse vectors. Particularly, this approach hierarchically groups the remaining of the feature vector sparse indication that leads to a VHAR. By exploiting the SIFT descriptors calculated on multiple scales, as well as dense grid and spatial information were taking into consideration. Finally, the proposed model attains better outcomes on contest datasets.

3. Developed Classification of Hep-2 Cell

The block diagram of the developed HEp-2 cell classification model is exhibited in Fig 1. Moreover, the process is described based on two schemes as classification as well as segmentation. An image I is used as the input for the process. At first, the image input is fed for the segmentation procedure, whereas the Hep-2 cells images are segmented. Therefore, two morphological operations are performed such as opening as well as closing.

To the classification process, the segmented image I_{sg} is subjected as the input and it is followed by the segmentation process, wherein the Hep-2 cells are classified for furthermore treatment. By deploying the CNN this is handled. In this paper, the main objective is to obtain accurate accuracy on the classification of the Hep-2 cells. In CNN the convolutional layer is optimally chosen to receive a maximum classification accuracy rate. By exploiting a novel optimization approach, the convolutional layer is optimally chosen.

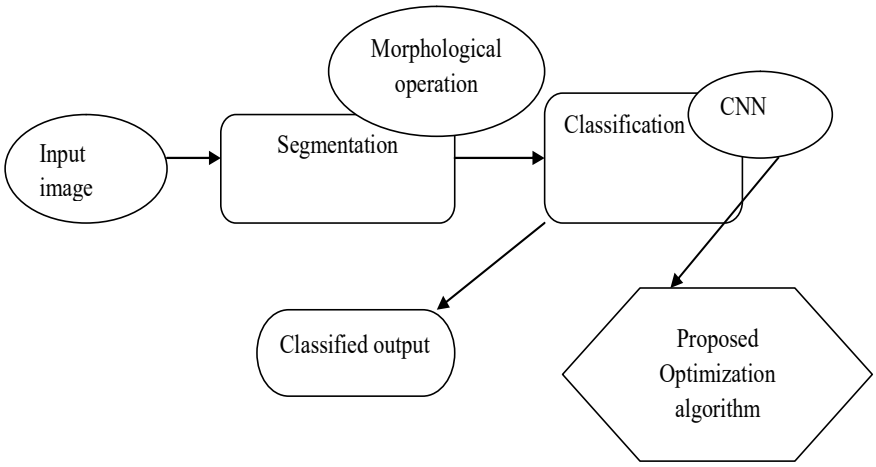

Fig.1. *Architecture model of adopted HEp-2 cell classification*

3.1 Morphology Segmentation

In the proposed model, the segmentation is considered as the initial procedure, wherein the I image is subjected as the input for the procedure. By exploiting the morphological operation, the segmentation process is carried out and that are described as below:

On the basis of set theory, morphological operations [6] are performed. Therefore, on the basis of the logical operations, they basically depend on which is simple to use. The fundamental operations of morphological operations are erosion as well as dilation. Moreover, the other operations namely opening as well as closing are performed by exploiting the 2 basic operators and are described as below:

(a) Opening: The image opening is the integration of both the dilation as well as erosion operations. Eq. (1) indicates that image E is opened by exploiting the G structuring element.

$$E \circ G = (E \Theta G) \oplus G \tag{1}$$

By exploiting the eq. (1), the correlation between the opening and erosion as well as dilation is explained. It explains the image erosion by exploiting the structuring element as well as the image that ensued is dilated by exploiting the same structuring element.

In the G structuring element, the opened image possesses the points boundary that attains the boundary E's extreme point as G is 'rolled' approximately within the boundary. Using the opening operation object smoothening summarization is performed, as well as it understands the narrow bridges and neglect minute expansions that happened in the object.

(b) Closing: In an image, the closing operation is an integration of both the operations namely dilation as well as erosion. By sense dilation order as well as erosion operation's incidence the difference amid the opening and closing operation is subjected. Using eq. (2), the image E closing operation by exploiting the structuring element G is shown.

$$E.G = (E \oplus G) \Theta G \tag{2}$$

The aforesaid statement indicates the correlation amid the closing utilizing erosion as well as dilation operation. Using equivalent structured element closing operation is explained as image E dilation with G structuring element, and the ensuing image is eroded.

The point is that the structuring element G which obtains the extreme point of E's boundary whilst G is 'rolled' against E regarding their boundary is subjected as the boundary of the closed image. The contours section smoothes by closing operation it usually concatenates the narrow breaks as well as thin fissures. Hence, using closing operation, in the object boundaries, the small holes and fill gaps are eradicated. This process output is a segmented image I_{sg}.

3.2. CNN Based Classification of Hep-2 Cells

The next process of the developed technique is the classification model in that the CNN is exploited to classify the segmented images [12]. The procedure is explained as follows:
Although with the NNs, the computer vision tasks are used, the previous knowledge integrated within the network model is an advantage task for better simplification performance. The most important contribution of the CNN [7], the spatial information practice amid the image pixel, and therefore it is on the basis of the discrete convolution [10].

Convolution: In eq. (3), using the function an image is stated. L indicates image which is shown by an array of size $a_1 \times a_2$. Eq. (4) indicates the filter, which is given as $P \in \Re^{2s_1+1\times 2s_2+1}$ the L image's discrete convolution beside with filter P, Eq. (5) indicates the filter P.

$$L : \{1,..., a_1\} \times \{1,...., a_2\} \to Z \subseteq \Re, (i, j) \mapsto L_{i,j} \tag{3}$$

$$(L * P)_{g,h} := \sum_{d=-s_1}^{s_1} \sum_{d=-s_2}^{s_2} P_{d,e} L_{g+d,h+e} \tag{4}$$

$$P = \begin{pmatrix} P_{-s_1,-s_2} & ..... & P_{-s_1,s_2} \\ : & P_{0,0} & : \\ P_{s_1,-s_2} & ..... & P_{s_1,s_2} \end{pmatrix} \tag{5}$$

Eq. (6) indicates the discrete Gaussian filter $P_{F(\sigma)}$ which is the usually exploited filter for smoothing, σ indicates the standard deviation of Gaussian distribution.

$$(P_{F(\sigma)})_{g,h} = \frac{1}{\sqrt{2\pi\sigma^2}} \exp\left(\frac{g^2 + h^2}{2\sigma^2}\right) \tag{6}$$

Layers: In CNN, several types of layers are established. Complex architectures have been constructed by stacking multiple layers as used for classification is made based on these layers.

Convolutional Layer: Let cl indicates Convolutional layer. Then, from preceding layers, the feature maps $\bar{r}_1^{(cl-1)}$ are obtained each size $\bar{r}_2^{(cl-1)} \times \bar{r}_3^{(cl-1)}$ comprises of the input of the layer cl. While $cl = 1$, the input is taken into consideration as the single image cl which is collected of "1" or more channels, by that the raw images are established as input in CNN. The cl layer possesses the output which involves $\bar{r}_1^{cl}$ feature maps of size $\bar{r}_2^{cl} \times \bar{r}_3^{cl}$. Eq. (7) indicates the evaluation of $\hat{X}_i^{cl}$ which states the i^{th} feature map in the layer cl.

$$\hat{X}_i^{cl} = D_i^{(cl)} + \sum_{j=1}^{\bar{r}_1^{(cl-1)}} P_{i,j}^{(cl)} * \hat{X}_j^{(cl-1)} \tag{7}$$

where $D_i^{(cl)}$ indicates bias matrix and the filter of size $2s_1^{cl} + 1 \times 2s_2^{cl} + 1$ relating with the j^{th} feature map in a layer $cl-1$ beside with feature map in the layer cl is indicated as $P_{i,j}^{(cl)}$. As aforesaid, border effects weight $\bar{r}_2^{cl}$ and $\bar{r}_3^{cl}$ is stated. Eq. (8) states the output feature map and its size is represented.

$$\bar{r}_2^{cl} = \bar{r}_2^{(cl-1)} - 2s_1^{cl} \text{ and } \quad \bar{r}_3^{cl} = \bar{r}_3^{(cl-1)} - 2s_2^{cl} \tag{8}$$

Often, the filters exploited for the calculation of fixed feature maps $\hat{X}_i^{cl}$ are the same, that is $P_{i,j}^{(cl)} = P_{i,k}^{(cl)}$ for $j \neq k$.

In layer, cl each feature map $\hat{X}_i^{cl}$ consists $\bar{r}_2^{cl} . \bar{r}_3^{cl}$ units arranged in the manner of a 2-dimensional array. In Eq. (9) and (10), the output is computed based on the unit at location (g,h). Wherein $D_i^{(cl)}$ indicates bias matrix and $\hat{X}_j^{(cl-1)}$ indicates the network trainable weight. By exploiting the sub-sampling the skipping factors u_1^{cl} and u_2^{cl} can be performed. The basic data is on fixing a number of pixels in

horizontal as well as the vertical direction, once prior to filter application. Eq. (11) states feature maps output size by exploiting skipping factors.

$$(\hat{X}_i^{cl})_{g,h} = (D_i^{(cl)})_{g,h} + \sum_{j=1}^{\bar{r}_1^{(cl-1)}} (P_{i.j}^{(cl)} * \hat{X}_j^{(cl-1)})_{g,h} \tag{9}$$

$$= D_i^{(cl)})_{g,h} + \sum_{j=1}^{\bar{r}_1^{(cl-1)}} \sum_{d=-s_1^{cl}}^{s_1^{cl}} \sum_{e=-s_2^{cl}}^{s_2^{cl}} (P_{i.j}^{(cl)})_{d,e} (\hat{X}_j^{(cl-1)})_{g+d,,h+e} \tag{10}$$

$$\bar{r}_2^{cl} = \frac{\bar{r}_2^{(cl-1)} - 2s_1^{cl}}{u_1^{cl} + 1} \text{ and } \bar{r}_3^{cl} = \frac{\bar{r}_3^{(cl-1)} - 2s_2^{cl}}{u_2^{cl} + 1} \tag{11}$$

Non-Linearity Layer: Suppose that cl be a layer, which is a non-linearity layer, whereas $\bar{r}_1^{cl}$ feature maps as the input and the result collected once more with $\bar{r}_1^{cl} = \bar{r}_1^{(cl-1)}$ feature maps, stated size of each as $\bar{r}_2^{(cl-1)} \times \bar{r}_3^{(cl-1)}$, and it is signified in Eq. (12). By exploiting eq. (13), the supplementary increase coefficient is stated.

$$\hat{X}_i^{cl} = f(\hat{X}_i^{(cl-1)}) \tag{12}$$

$$\hat{X}_i^{cl} = ga_i f(\hat{X}_i^{(cl-1)}) \tag{13}$$

Rectification: Let cl be the rectification layer. For each module, as per Eq. (14), the absolute value of feature maps is calculated and the input comprises of $\bar{r}_1^{(cl-1)}$ feature map of size $\bar{r}_2^{(cl-1)} \times \bar{r}_3^{(cl-1)}$, wherein the absolute value is estimated as pointwise, therefore output includes $\bar{r}_1^{cl} = \bar{r}_1^{(cl-1)}$ feature maps not enhanced in size.

$$\hat{X}_i^{cl} = \left| \hat{X}_i^{cl} \right| \tag{14}$$

Local Contrast Normalization Layer: Suppose that cl as the contrast normalization layer. The local contrast normalization layer's most important intention is to compel local competition amid nearby units within feature maps as well as units within an alike spatial location in a variety of feature maps. Provided feature maps of size $\bar{r}_2^{(cl-1)} \times \bar{r}_3^{(cl-1)}$ as $\bar{r}_1^{(cl-1)}$, $\bar{r}_1^{cl} = \bar{r}_1^{(cl-1)}$ feature maps are included in the output of layer cl with un-adjustment in size. By exploiting eq. (15), the subtractive normalization operation computation is shown. As per Eq. (16), the output of the layer cl is presented, wherein, K and μ indicates hyper-parameters.

$$(\hat{X}_i^{cl})_{g,h} = \hat{X}_i^{(cl-1)} - \sum_{j=1}^{\bar{r}^{(cl-1)}} P_{F(\sigma)} * \hat{X}_j^{(cl-1)} \tag{15}$$

$$(\hat{X}_i^{cl})_{g,h} = \frac{(\hat{X}_i^{(cl-1)})_{g,h}}{\left(K + \mu \sum_{j=1}^{\bar{r}_1^{cl-1}} (\hat{X}_i^{(cl-1)})_{g,h}^2 \right)^{\mu}} \tag{16}$$

Subsampling layer as well as Feature Pooling: Let cl represents pooling layer, as well as their outputs, contain $\bar{r}_1^{cl} = \bar{r}_1^{(cl-1)}$ feature maps of reduced size. In general, the pooling estimates in each feature map by positioning the windows at over-lapping locations as well as preserving one value for each window, therefore that feature maps sub-sampling is performed. Moreover, 2 types of pooling are distinguished as below:

In ,max-pooling represents the maximum value of each window is taken into consideration and it is indicated as Q_{Max}. While the boxcar filter is exploited, the average Pooling operation and is indicated as Q_{Ag}.

Fully Connected Layer: Suppose that the fully connected layer is represented as cl. "If the layer $cl-1$ is not fully connected, subsequently layer cl uses input other than $\bar{r}_1^{(cl-1)}$ feature maps of size $\bar{r}_2^{(cl-1)} \times \bar{r}_3^{(cl-1)}$ as well as j layer with i^{th} the unit is estimated based on Eq. (17)".

$$\hat{x}_i^{cl} = f(v_i^{cl}) \text{ with } v_i^{cl} = \sum_{j=1}^{\bar{r}_1^{cl-1}} \sum_{g=1}^{\bar{r}_2^{cl-1}} \sum_{h=1}^{\bar{r}_3^{cl-1}} W_{i,j,g,h}^{cl} \left(\hat{X}_j^{(cl-1)} \right) \tag{17}$$

Wherein weight-related with the unit at a location (g,h) in the j^{th} layer feature map $cl-1$ as well as i^{th} unit in the layer cl is indicated as $W_{i,j,g,h}^{cl}$. Subsequent to the CNN process the ensuing output is the classified image.

4. Proposed Hybrid PSO-JA for Convolutional Layer Optimization

The major objective of the developed Hep-2 Classification technique is reserved in the achievement of competent classification accuracy. Actually, to avoid the local optima CNN depends on the initial parameter tuning.

Therefore, CNN needs an important number of works they required for starting the issue, and it requires a little specialized knowledge in that domain. To surmount these problems, this paper tries to use a few adaptive schemes on CNN by exploiting the optimization idea. Hence, a hybrid approach named Hybrid PSO-JA is used for optimizing the convolutional layer of CNN. Furthermore, the objective model of the developed technique is shown in Eq. (18).

$$OB = \text{Min}(E) \tag{18}$$

Wherein E indicates the error amid the actual as well as the predicted value.

4.1. Adopted Hybrid PSO-JA

The adopted hybrid optimization approach integrates the advantages of both the PSO [8] [11] as well as Jaya algorithm [9]. It improves search space, and it force solution to attain the global optimal solution as well as far from worst solutions.

The proposed model updating formulation is devised in eq. (19). It is based upon the global optimal, worst solution and considering the effect of self-experience of related particles.

$$x_{k+1} = v_k x_k + c_1 \times r_1 \times \left(x_k^{best} - x_k\right) - c_2 \times r_2 \times \left(x_k^{worst} - x_k\right) + c_3 \times x_3 \times \left(x_k^{gbest} - x_k\right) \tag{19}$$

Where x_k^{gbest} indicates the variable k value for a global member of a set of probable solutions. For k^{th} iteration within range of (0, 1). c_1, c_2 as well as c_3 indicates learning coefficients, the initial term exhibits similarity of the solution to move closer to the individual optimal solution, r_1, r_2 and r_3 indicates the 3 arbitrary numbers for the k^{th} variable. The next term indicates the the similarity of the solution to move closer to the global optimal solution as well as the final term is the propensity of the solution to keep away from the worst solution. The below steps explains the process of the proposed Hybrid PSO-JA model.

a) Initializes all the parameters of the algorithm
b) Generate the first population of N particles
c) Calculate the best and worst solutions
d) Compute each particle of an initialized variable by ascertaining fitness eq. (18).
e) Recognize personal, global, as well as worst solutions.
f) By exploiting the eq. (19), update the variables.

5. Result Analysis

The experimentation analysis of the adopted method over the conventional model was demonstrated. Here, 4 test cases were exploited. Furthermore, the experimentation was performed by exploiting the positive as well as negative metrics. Here, the proposed method was compared with the conventional models such as Particle Swarm Optimization (PSO), Firefly (FF), Genetic Algorithm (GA), Whale Optimization Algorithms (WOA).

Fig 2, 3, 4, and 5 demonstrate the analysis of the adopted model with conventional techniques regarding the positive as well as negative metrics for 4 test cases. In Fig 2, the proposed model is 12% better than the PSO, 22% better than the FF, 22% better than the GA, and 22% better than the WOA for accuracy. In Fig 3, the proposed model is 21% better than the PSO, 16% better than the FF, 18% better than the GA, and 19% better than the WOA for accuracy. In Fig 4, the proposed model is 14% better than the PSO, 18% better than the FF, 22% better than the GA, and 19% better than the WOA for accuracy. The resultant analysis of positive measures such as accuracy, specificity, and precision shows the superiority of the proposed model over the other conventional techniques.

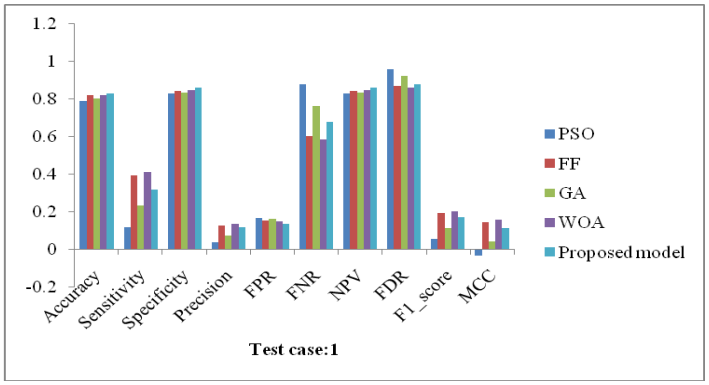

Fig.2. Analysis of adopted method over the existing models for Test Case: 1

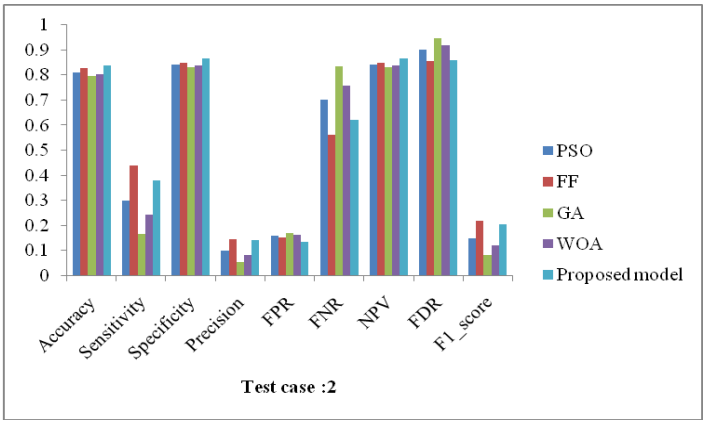

Fig.3. Analysis of adopted method over the existing techniques for a Test case:2

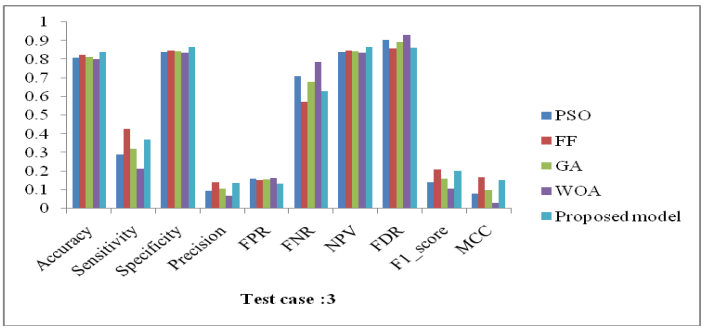

Fig.4. Analysis of adopted method over the existing models for Test case:3

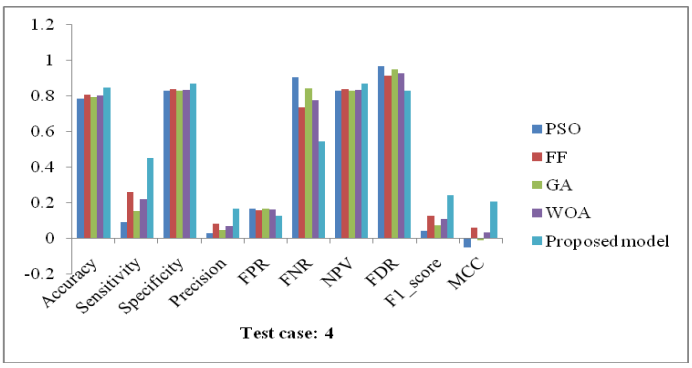

Fig.5. Analysis of adopted method over the existing models for Test case: 4

6. Conclusion

In this research, a new HEp-2 classification procedure was performed by using two operations, such as classifications as well as segmentation. Initially, the Ep-2 cells segmentation was performed by exploiting the morphological operation such as opening as well as closing. Subsequent to the segmentation procedure, using the enhanced CNN, the classification was performed. The main contribution of effectual classification of HEp-2 cells was developed by using a novel optimization Hybrid PSO-JA concept. Furthermore, in CNN, the convolutional layer was optimized by exploiting a novel Hybrid PSO-JA approach. At last, the developed technique was evaluated with the conventional models and therefore it shows the superiority of the proposed model regarding the classification- precise.

Compliance with Ethical Standards

Conflicts of interest: Authors declared that they have no conflict of interest.

Human participants: The conducted research follows the ethical standards and the authors ensured that they have not conducted any studies with human participants or animals.

Reference

[1] LinRuitao LuWenmin Fu,"IFNgamma-inducible CXCL10/CXCR3 axis alters the sensitivity of HEp-2 cells to ionizing radiation", Experimental Cell Research, 28 November 2020.

[2] Zohreh KhodaiiSolat EslamiMahboobeh Mehrabani Natanzi,"Evaluation of aqueous-extracts from four aromatic plants for their activity against Candida albicans adhesion to human HEp-2 epithelial cells", Gene Reports, 5 November 2019.

[3] Khamael Al-DulaimiVinod ChandranInmaculada Tomeo-Reyes,"Benchmarking HEp-2 specimen cells classification using linear discriminant analysis on higher order spectra features of cell shape", Pattern Recognition Letters, 21 June 2019.

[4] Larissa Ferreira RodriguesMurilo Coelho NaldiJoão Fernando Mari," Comparing convolutional neural networks and preprocessing techniques for HEp-2 cell classification in immunofluorescence images", Computers in Biology and Medicine20 November 2019.

[5] Dimitris KastaniotisFoteini FotopoulouSpiros Fotopoulos,"HEp-2 cell classification with Vector of Hierarchically Aggregated Residuals", Pattern Recognition, May 2017.

[6] Srisha, Ravi and Khan, Am, Morphological Operations for Image Processing, Understanding and its Applications, 2013.

[7] O'Shea, Keiron and Nash, Ryan, An Introduction to Convolutional Neural Networks, ArXiv e-prints, 2015.

[8] El-Sehiemy RA EM, Abd-Elwanis MI, Kotb AB. Synchronous motor design using particle swarm optimization technique. In: Proceedings of the 14th international Middle East power systems conference (MEPCON'10). Cairo University; 2010. p. 795–800.

[9] Huang C, Wang L, Yeung RSC, Zhang Z, Chung HSH, Bensoussan A. A prediction model-guided Jaya algorithm for the PV system maximum power point tracking. IEEE Trans Sustain Energy 2018;9(1):45–55.

[10] Subramonian Krishna Sarma. "Optimally Configure Deep Convolutional Neural Network for Attack Detection in Internet of Things: Impact of Algorithm of the Innovative Gunner", Wireless Personal Communications, 2021.

[11] Heyan Zhang,"Secure Routing Protocol using Salp-Particle Swarm Optimization Algorithm",Journal of Networking and Communication Systems,vol. 3, no.3, July 2020.

[12] Vaibhav Ankush Thorat,"Cloud Intrusion Detection using Modified Crow Search Optimized based Neural Network",Journal of Networking and Communication Systems,vol. 3, no.3, July 2020.